Investigation of Nonlinear Bending Analysis of Moderately Thick Functionally Graded Material Sector Plates Subjected to Thermomechanical Loads by the GDQ Method

Farhad Alinaghizadeh[1] and Mehran Kadkhodayan[2]

Abstract: Large deflection analysis of functionally graded annular sector plates subjected to thermomechanical loads is presented. Based on the first-order shear deformation theory in conjunction with nonlinear von Kármán assumptions, the governing system of equations is derived. A polynomial-based generalized differential quadrature (GDQ) method is used to discretize the nonlinear governing equations. The Newton-Raphson algorithm is then employed to solve the system of nonlinear algebraic equations. Material properties of the plates are assumed to depend on temperature and are graded in the thickness direction based on a simple power-law distribution. Based on a comparison of results obtained for plates with temperature-dependent material properties versus plates with temperature-independent material properties, it is found that the effects of temperature dependency cannot be neglected. Furthermore, the effects of temperature rise, material index, thickness-to-radius ratio, and temperature dependency of material are studied in detail. **DOI: 10.1061/(ASCE)EM.1943-7889.0000715.**

Author keywords: Sector plat; Nonlinear bending analysis; Thermomechanical loads; Generalized differential quadrature; Functionally graded material.

Introduction

Functionally graded materials (FGMs) have received much attention since their introduction in 1984 by a group of material scientists in Japan (Yamanoushi et al. 1990; Koizumi 1993). These advanced materials are microscopically heterogeneous, and their mechanical properties vary continuously in at least one direction. FGMs are usually made of metal and ceramic. The metal component precludes fracture, and the ceramic component has low thermal conductivity and enables the material to withstand high-temperature environments.

Because an analytical close-form solution is limited to some simple problems, semianalytical and numerical methods are introduced. The generalized differential quadrature (GDQ) method (Shu and Richards 1992) is a numerical method with high accuracy based on employing a few number of grid points, which leads to less computational effort. The GDQ method is a new version of differential quadrature method (DQM) that was introduced by Bellman and Casti (1971). Finding appropriate weighting coefficients has been the fundamental issue in this method, and the main dissimilarity between the GDQ method and prior versions is the method of obtaining weighting coefficients.

Thin-walled structures such as plates and shells are used extensively in many industrial fields. Most notably, circular and annular sector plates made of FGM have numerous applications in mechanical, civil, aerospace, and other industrial and engineering fields. The issue of analysis of annular sector plates has become a cause célèbre among researchers since the first study carried out by Nádai (1915). Nonetheless, studies on annular sector plates in comparison with rectangular plates are infrequent. Aghdam et al. (2007) used the extended Kantorovich method (EKM) for bending analysis of fully clamped annular sector plates subjected to both uniform and nonuniform loads. In another work of Aghdam et al. (2012), moderately thick, fully clamped annular sector plates made of FGM were considered. Andakhshideh et al. (2010) studied nonlinear bending analysis of laminated annular sector plates with various boundary conditions by the GDQ method. Salehi and Turvey (1991) used the dynamic relaxation (DR) method to determine the nonlinear response of annular sector plates. In another work, Salehi and Shahidi (1994) implemented the same method for large deflection analysis of moderately thick sector plates. Nath et al. (2005) investigated nonlinear bending analysis of moderately thick sector plates. Jomehzadeh et al. (2009) decoupled and solved equilibrium equations for moderately thick functionally graded sector plates by introducing an analytical solution. Saidi and Hasani Baferani (2010) used the analytical solution for thermal buckling analysis of moderately thick functionally graded sector plates. More recently, Naderi and Saidi (2011) investigated the stability of annular sector plates with the analytical method. Some researchers have also studied functionally graded annular sector plates whose mechanical properties vary in the radius direction. These plates are known as radially functionally graded (RFG) plates. Mousavi and Tahani (2012) studied the bending of RFG sector plates with various boundary conditions. Hosseini-Hashemi et al. (2010a) used the DQM to study buckling of RFG circular and sector plates resting on elastic foundations. In another work, Hosseini-Hashemi et al. (2010b) employed the DQM for vibration analysis of RFG plate annular sectors with variable thicknesses.

Furthermore, numerous studies on the thermal bending of functionally graded rectangular plates are available. Praveen and Reddy (1998) studied the nonlinear static and dynamic responses of functionally graded plates subjected to both mechanical and thermal

[1]Dept. of Mechanical Engineering, Ferdowsi Univ. of Mashhad, Mashhad 9177948974, Iran. E-mail: Farhad.Alinaghi.zadeh@gmail.com

[2]Professor, Dept. of Mechanical Engineering, Ferdowsi Univ. of Mashhad, Mashhad 9177948974, Iran (corresponding author). E-mail: kadkhoda@um.ac.ir

Note. This manuscript was submitted on April 15, 2013; approved on September 24, 2013; published online on September 26, 2013. Discussion period open until June 9, 2014; separate discussions must be submitted for individual papers. This paper is part of the ***Journal of Engineering Mechanics***, © ASCE, ISSN 0733-9399/04014012(11)/$25.00.

loads by the FEM. Na and Kim (2006) investigated the nonlinear bending of fully clamped functionally graded rectangular plates subjected to transverse uniform pressure and thermal loads by the three-dimensional (3D) FEM. In some studies, the material properties were assumed to depend on temperature. Yang and Shen (2003) studied the nonlinear response of functionally graded plates with temperature-dependent material properties subjected to thermomechanical loads. The nonlinear bending of functionally graded plates with temperature-dependent material properties resting on elastic foundations was studied by Shen and Wang (2010).

Although FGMs basically were introduced as thermal barrier materials and are used in high-temperature environments, based on a review of the available literature, it appears that most studies on annular sector plates are confined to plates subjected to mechanical, not thermal loading. Thus far the authors have not encountered any paper dealing with nonlinear bending analysis of functionally graded annular sector plates with temperature-dependent material properties subjected to thermomechanical loads, and the results obtained from thermal bending analysis of annular sector plates may be used as a reference for future studies.

In this study, the nonlinear bending analysis of fully clamped functionally graded annular sector plates with temperature-dependent material properties is presented. Material properties are assumed to be a nonlinear function of temperature and are graded in the thickness direction based on a simple power-law distribution in terms of the volume fraction of the constituent. Employing the principle of minimum total potential energy, the governing equations are obtained based on the first-order shear deformation theory (FSDT) and von Kármán–type nonlinearity. The GDQ method in conjunction with the Newton-Raphson iterative scheme is then used to solve the system of five nonlinear governing equations. It is shown that solutions of the GDQ method are in excellent agreement with results of other numerical methods. It is found that analysis of plates with temperature-independent material properties is inadequate for plates that are employed in high-temperature environments. Furthermore, the effects of temperature increases, the volume fraction exponent, inner-to-outer-radii ratios, and radius-to-thickness ratios are discussed in detail.

Material Properties

Consider a fully clamped functionally graded annular sector plate with inner radius of r_i, outer radius of r_o, uniform thickness of h, and total angle of α, as shown in Fig. 1. It is assumed that the material properties of the plates vary through the thickness direction based on a function of properties and volume fractions of the constituent. This can be expressed as

$$P = P_c V_c + P_m V_m \tag{1}$$

where P_c and P_m = material properties of ceramic and metal, respectively; V_c and V_m = volume fraction of the constituent material and, based on a simple power-law distribution, are considered as follows:

$$V_c(z) = \left(\frac{z}{h} + \frac{1}{2}\right)^n \tag{2a}$$

$$V_m(z) = 1 - V_c(z) \tag{2b}$$

where n = volume-fraction index or material index, and takes values greater than or equal to zero. The thermal and mechanical properties of FGMs change significantly with temperature (Reddy and Chin 1998). For example, Young's modulus of stainless steel, nickel, Ti-6Al-4V, and zirconia are reduced by 37, 21, 34, and 31%, respectively, when the temperature increases from room temperature

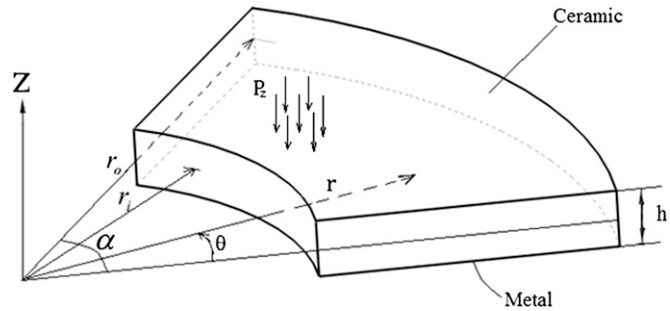

Fig. 1. Geometry and coordinate system of annular sector plate

to 1,000 K (Yang and Shen 2003). Therefore, Young's modulus E_m and E_c, thermal expansion coefficients α_m and α_c, and thermal conductivity coefficients K_m and K_c are assumed to be functions of temperature. Hence E, α, and K depend on both temperature and position and are written as

$$E(z,T) = \left[E_c(T) - E_m(T)\right]\left(\frac{z}{h} + \frac{1}{2}\right)^n + E_m(T) \tag{3a}$$

$$\alpha(z,T) = \left[\alpha_c(T) - \alpha_m(T)\right]\left(\frac{z}{h} + \frac{1}{2}\right)^n + \alpha_m(T) \tag{3b}$$

$$K(z,T) = \left[K_c(T) - K_m(T)\right]\left(\frac{z}{h} + \frac{1}{2}\right)^n + K_m(T) \tag{3c}$$

The effect of changing Poisson's ratio υ on the mechanical behavior of the functionally graded plates is very small (Chi and Chung 2006a, b); therefore, it can be assumed to be constant.

Temperature Field

The nonuniform temperature gradient $T(z)$ is assumed to vary along the thickness direction and is obtained by solving the following heat-transfer equation:

$$\frac{d}{dz}\left[K(z,T)\frac{dT(z)}{dz}\right] = 0 \tag{4}$$

By denoting the temperature at the top surface as $T(h/2) = T_c$ and at bottom surface as $T(-h/2) = T_m$, temperature distribution is obtained from Eq. (4) as

$$T(z) = T_m + (T_c - T_m)\int_{-h/2}^{z}\frac{dz}{K(z,T)}\Bigg/\int_{-h/2}^{h/2}\frac{dz}{K(z,T)} \tag{5}$$

where $T(z)$ is measured from the stress-free state. It should be noted that $T(z)$ is obtained by dividing the thickness into several layers and calculating the integral of $1/K(z,T)$ from $-h/2$ to each layer. Temperature profiles for FGM plates with a temperature increase of $\Delta T = 300$ and material indices of $n = 0.3$ and $n = 2$ are shown in Fig. 2. It can be seen that variations in temperature through thickness are nonlinear.

Governing Equations

The displacement components of an arbitrary point within a plate, in polar coordinate (r, θ, z) based on the FSDT (Wang et al. 2000), are given by

$$U(r,\theta,z) = u(r,\theta) + z\varphi_r(r,\theta) \tag{6a}$$
$$V(r,\theta,z) = v(r,\theta) + z\varphi_\theta(r,\theta) \tag{6b}$$
$$W(r,\theta,z) = w(r,\theta) \tag{6c}$$

where u, v, and w = displacements of a point at the middle surface (i.e., $z = 0$) along the r-, θ-, and z-coordinates, respectively; and φ_r and φ_θ = rotations about θ- and r-axes. Introducing the displacement field into the von Kármán nonlinear strain-displacement equation (Wang et al. 2000), the nonlinear strain component can be derived as

$$\varepsilon_r = \frac{\partial u}{\partial r} + \frac{1}{2}\left(\frac{\partial w}{\partial r}\right)^2 + z\frac{\partial \varphi_r}{\partial r} \tag{7a}$$
$$\varepsilon_\theta = \frac{1}{r}\left(\frac{\partial v}{\partial \theta} + u\right) + \frac{1}{2r^2}\left(\frac{\partial w}{\partial \theta}\right)^2 + \frac{z}{r}\left(\frac{\partial \varphi_\theta}{\partial \theta} + \varphi_r\right) \tag{7b}$$
$$\varepsilon_z = 0 \tag{7c}$$
$$2\varepsilon_{r\theta} = \frac{\partial v}{\partial r} + \frac{1}{r}\frac{\partial u}{\partial \theta} - \frac{v}{r} + \frac{1}{r}\frac{\partial w}{\partial r}\frac{\partial w}{\partial \theta} + z\left(\frac{\partial \varphi_\theta}{\partial r} + \frac{1}{r}\frac{\partial \varphi_r}{\partial \theta} - \frac{\varphi_\theta}{r}\right) \tag{7d}$$
$$2\varepsilon_{rz} = \frac{\partial w}{\partial r} + \varphi_r \tag{7e}$$
$$2\varepsilon_{\theta z} = \frac{1}{r}\frac{\partial w}{\partial \theta} + \varphi_\theta \tag{7f}$$

Considering the plane-stress state, the constitutive equations are written as

$$\sigma_r = \frac{E(z,T)}{1-\nu^2}\left[\varepsilon_r + \nu\,\varepsilon_\theta - \alpha(z,T)T(z)(1+\nu)\right] \tag{8a}$$
$$\sigma_\theta = \frac{E(z,T)}{1-\nu^2}\left[\varepsilon_\theta + \nu\,\varepsilon_r - \alpha(z,T)T(z)(1+\nu)\right] \tag{8b}$$
$$\sigma_{r\theta} = \frac{E(z,T)}{2\,(1+\upsilon)}(2\,\varepsilon_{r\theta}) \tag{8c}$$
$$\sigma_{rz} = \frac{E(z,T)}{2\,(1+\upsilon)}(2\,\varepsilon_{rz}) \tag{8d}$$
$$\sigma_{\theta z} = \frac{E(z,T)}{2\,(1+\upsilon)}(2\,\varepsilon_{\theta z}) \tag{8e}$$

where quantities σ_r, σ_θ and $\sigma_{r\theta}$, $\sigma_{\theta z}$, and σ_{rz} = components of normal and shear stresses, respectively. By employing the principle of minimum total potential energy (Reddy 2002), the equilibrium equations are obtained as

$$\delta u\colon\ \frac{\partial N_r}{\partial r} + \frac{1}{r}\frac{\partial N_{r\theta}}{\partial \theta} + \frac{N_r - N_\theta}{r} = 0 \tag{9a}$$
$$\delta v\colon\ \frac{\partial N_{r\theta}}{\partial r} + \frac{1}{r}\frac{\partial N_\theta}{\partial \theta} + \frac{2}{r}N_{r\theta} = 0 \tag{9b}$$
$$\delta w\colon\ \frac{\partial Q_r}{\partial r} + \frac{1}{r}\frac{\partial Q_\theta}{\partial \theta} + \frac{1}{r}Q_r + N_1 = P_z \tag{9c}$$
$$\delta \varphi_r\colon\ \frac{\partial M_r}{\partial r} + \frac{\partial M_{r\theta}}{r\,\partial \theta} + \frac{M_r - M_\theta}{r} - Q_r = 0 \tag{9d}$$
$$\delta \varphi_\theta\colon\ \frac{\partial M_{r\theta}}{\partial r} + \frac{\partial M_\theta}{r\,\partial \theta} + \frac{2}{r}M_{r\theta} - Q_\theta = 0 \tag{9e}$$

where P_z = applied external pressure function on upper surface of the plate; and N_1 is defined as follows:

$$N_1 = N_r\frac{\partial^2 w}{\partial r^2} + N_\theta\left(\frac{1}{r}\frac{\partial w}{\partial r} + \frac{1}{r^2}\frac{\partial^2 w}{\partial \theta^2}\right) + 2N_{r\theta}\left(\frac{1}{r}\frac{\partial^2 w}{\partial r\,\partial \theta} - \frac{1}{r^2}\frac{\partial w}{\partial \theta}\right) \tag{10}$$

where N_r, N_θ, and $N_{r\theta}$ = in-plane force resultants; Q_r and Q_θ = out-of-plane force resultants; and M_r, M_θ, and $M_{r\theta}$ = bending and twisting resultants, respectively, and are defined as

$$(N_r, N_\theta, N_{r\theta}) = \int_{-h/2}^{h/2} (\sigma_r, \sigma_\theta, \sigma_{r\theta})\,dz \tag{11a}$$
$$(Q_r, Q_\theta) = K^2\int_{-h/2}^{h/2} (\sigma_{rz}, \sigma_{\theta z})\,dz \tag{11b}$$
$$(M_r, M_\theta, M_{r\theta}) = \int_{-h/2}^{h/2} z\,(\sigma_r, \sigma_\theta, \sigma_{r\theta})\,dz \tag{11c}$$

where K^2 = shear correction factor, in this study assumed to be $5/6$ (Nguyen et al. 2008). On substitution of Eqs. (7) and (8) into Eq. (11), stress and moment resultants can be written as

$$\{F\} = [C]\{U\} - \{F_1\} \tag{12}$$

where

$$\{F\} = \{N_r, N_\theta, N_{r\theta}, M_r, M_\theta, M_{r\theta}, Q_r, Q_\theta\}^T \tag{13a}$$

$$[C] = \begin{bmatrix} A_{11} & A_{12} & 0 & B_{11} & B_{12} & 0 & 0 & 0 \\ A_{12} & A_{11} & 0 & B_{12} & B_{11} & 0 & 0 & 0 \\ 0 & 0 & A_{33} & 0 & 0 & B_{33} & 0 & 0 \\ B_{11} & B_{12} & 0 & D_{11} & D_{12} & 0 & 0 & 0 \\ B_{12} & B_{11} & 0 & D_{12} & D_{11} & 0 & 0 & 0 \\ 0 & 0 & B_{33} & 0 & 0 & D_{33} & 0 & 0 \\ 0 & 0 & 0 & 0 & 0 & 0 & A_{33} & 0 \\ 0 & 0 & 0 & 0 & 0 & 0 & 0 & A_{33} \end{bmatrix} \tag{13b}$$

$$\{U\} = \begin{Bmatrix} \dfrac{\partial u}{\partial r} + \dfrac{1}{2}\left(\dfrac{\partial w}{\partial r}\right)^2 \\ \dfrac{1}{r}\dfrac{\partial v}{\partial \theta} + \dfrac{u}{r} + \dfrac{1}{2}\left(\dfrac{1}{r}\dfrac{\partial w}{\partial \theta}\right)^2 \\ \dfrac{1}{r}\dfrac{\partial u}{\partial \theta} + \dfrac{\partial v}{\partial r} - \dfrac{v}{r} + \dfrac{1}{r}\dfrac{\partial w}{\partial \theta}\dfrac{\partial w}{\partial r} \\ \dfrac{\partial \varphi_r}{\partial r} \\ \dfrac{1}{r}\dfrac{\partial \varphi_\theta}{\partial \theta} + \dfrac{\varphi_r}{r} \\ \dfrac{1}{r}\dfrac{\partial \varphi_r}{\partial \theta} + \dfrac{\partial \varphi_\theta}{\partial r} - \dfrac{\varphi_\theta}{r} \\ K^2\left(\varphi_r + \dfrac{\partial w}{\partial r}\right) \\ K^2\left(\varphi_\theta + \dfrac{1}{r}\dfrac{\partial w}{\partial \theta}\right) \end{Bmatrix} \tag{13c}$$

$$\{F_1\} = \{N_r^T, N_\theta^T, 0, M_r^T, M_\theta^T, 0, 0, 0\}^T \tag{13d}$$

where the constants are the stiffness coefficients and can be computed as

$$(A_{11}, B_{11}, D_{11}) = \int_{-h/2}^{h/2} \frac{E(z,T)}{1-\upsilon^2}(1, z, z^2)\,dz \tag{14a}$$

$$(A_{12}, B_{12}, D_{12}) = \int_{-h/2}^{h/2} \frac{\nu E(z,T)}{1-\upsilon^2}(1, z, z^2)dz \tag{14b}$$

$$(A_{33}, B_{33}, D_{33}) = \int_{-h/2}^{h/2} \frac{E(z,T)}{2(1+\upsilon)}(1, z, z^2)dz \tag{14c}$$

Furthermore, thermal terms are defined as

$$N_r^T = N_\theta^T = \int_{-h/2}^{h/2} \frac{E(z,T)}{1-\upsilon}\alpha(z,T)T(z)dz \tag{15a}$$

$$M_r^T = M_\theta^T = \int_{-h/2}^{h/2} z\frac{E(z,T)}{1-\upsilon}\alpha(z,T)T(z)dz \tag{15b}$$

On substitution of Eq. (12) into Eq. (9), the ultimate forms of governing equations in terms of displacements and rotations can be obtained; for the sake of brevity, the first equation is written as

$$\begin{aligned}&\frac{(A_{12}+A_{33})}{r^2}\frac{\partial w}{\partial\theta}\frac{\partial^2 w}{\partial r\,\partial\theta} + \frac{(A_{11}-A_{12})}{2r}\left(\frac{\partial w}{\partial r}\right)^2 + \frac{(-A_{11}-A_{12})}{2r^3}\left(\frac{\partial w}{\partial\theta}\right)^2 + A_{11}\frac{\partial w}{\partial r}\frac{\partial^2 w}{\partial r^2} + \frac{A_{33}}{r^2}\frac{\partial^2 w}{\partial\theta^2}\frac{\partial w}{\partial r} + A_{11}\frac{\partial^2 u}{\partial r^2} + \frac{A_{33}}{r^2}\frac{\partial^2 u}{\partial\theta^2} + \frac{A_{11}}{r}\frac{\partial u}{\partial r}\\ &+ \frac{-A_{11}}{r^2}u + \frac{(-A_{11}-A_{33})}{r^2}\frac{\partial v}{\partial\theta} + \frac{(A_{12}+A_{33})}{r}\frac{\partial^2 v}{\partial r\,\partial\theta} + B_{11}\frac{\partial^2\varphi_r}{\partial r^2} + \frac{B_{33}}{r^2}\frac{\partial^2\varphi_r}{\partial\theta^2} + \frac{B_{11}}{r}\frac{\partial\varphi_r}{\partial r} - \frac{B_{11}}{r^2}\varphi_r + \frac{(-B_{11}-B_{33})}{r^2}\frac{\partial\varphi_\theta}{\partial\theta}\\ &+ \frac{(B_{12}+B_{33})}{r}\frac{\partial^2\varphi_\theta}{\partial r\,\partial\theta} = 0\end{aligned} \tag{16}$$

Five partial differential equations in terms of displacements and rotations are solved in conjunction with the following clamped boundary conditions:

$$u = v = w = \varphi_r = \varphi_\theta = 0 \tag{17}$$

Application of the GDQ Method

In this section, a concise review of the GDQ method is presented. In the GDQ method, the partial derivative of a function with respect to a variable at a specific grid point is approximated as a weighted linear sum of the function values at all discrete points in the complete domain of that variable. To clear this concept, a one-dimensional function $f(x)$ on a domain $a \le x \le b$ is considered. Assuming that the domain is discretized by N grid points, the mth-order derivative of $f(x)$ at a discrete point x_i with respect to the x-direction can be written as

$$\left.\frac{d^m f(x)}{dx^m}\right|_{x=x_i} = \sum_{j=1}^{N} C_{ij}^{(m)} f(x_j) \quad i = 1, 2, \ldots, N \tag{18}$$

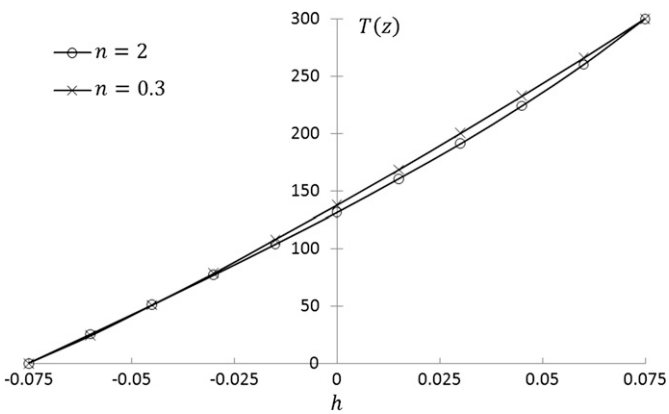

Fig. 2. Nonlinear variations of temperature versus thickness

Table 1. Comparison of Linear Maximum Deflection

	$10^4 wEh^4/[12(1-\nu^2)P_z r_o^4]$			
$n_r \times n_\theta$	$r_i/r_o = 0$	$r_i/r_o = 1/4$	$r_i/r_o = 1/2$	$r_i/r_o = 3/4$
9×9	2.8706	2.8356	1.4160	0.1038
11×11	2.8697	2.8318	1.4161	0.1020
13×13	2.8686	2.8340	1.4161	0.1020
Aghdam et al. (2007)	2.9100	2.8600	1.4200	0.1020
Mousavi and Tahani (2012)	—	2.8410	1.4257	0.1043

Table 2. Mechanical Properties of Constituent Materials

Properties	Metal: aluminum	Ceramic: alumina
Young's modulus	$E_m = 70$ GPa	$E_c = 380$ GPa
Poisson's ratio	$\nu_m = 0.3$	$\nu_c = 0.3$

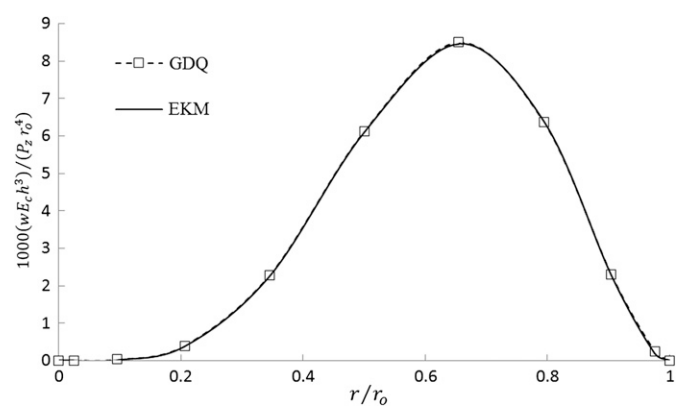

Fig. 3. Prediction of EKM (data from Aghdam et al. 2012) and GDQ method for linear deflection along centerline $(r, \alpha/2)$ of solid sector plate with $n = 2$

Table 3. Comparison of Deflection for Nonlinear Bending of Solid Sector Plates

$P_z/(Eh^4/r_o^4)$	w/h					
	$h/r_o = 0.05$			$h/r_o = 0.1$		
	Present	Nath et al. (2005)	Salehi and Shahidi (1994)	Present	Nath et al. (2005)	Salehi and Shahidi (1994)
100	0.3249	0.32484	0.3601	0.3940	0.39401	0.4576
200	0.5788	0.57860	0.6292	0.6672	0.66701	0.7544
300	0.7714	0.77103	0.8310	0.8620	0.86158	0.9629
400	0.9245	0.92389	0.9919	1.0133	1.01249	1.1246
500	1.0515	1.05078	1.1260	1.1376	1.13652	1.2580

Table 4. Comparison of Radial Moment Resultants for Nonlinear Bending of Solid Sector Plates

$P_z/(Eh^4/r_o^4)$	$M_r r_o^2/(Eh^4)$					
	$h/r_o = 0.05$			$h/r_o = 0.1$		
	Present	Nath et al. (2005)	Salehi and Shahidi (1994)	Present	Nath et al. (2005)	Salehi and Shahidi (1994)
100	0.9662	0.95753	0.9490	0.9398	0.91313	0.8810
200	1.6604	1.64170	1.5860	1.5129	1.47220	1.3830
300	2.1328	2.10337	2.0120	1.8932	1.82196	1.7110
400	2.4853	2.43229	1.9590	2.1579	2.06698	1.9590
500	2.7448	2.68104	2.5640	2.3630	2.25343	2.1600

Table 5. Comparison of Circumferential Moment Resultants for Nonlinear Bending of Solid Sector Plates

$P_z/(Eh^4/r_o^4)$	$M_\theta r_o^2/(Eh^4)$					
	$h/r_o = 0.05$			$h/r_o = 0.1$		
	Present	Nath et al. (2005)	Salehi and Shahidi (1994)	Present	Nath et al. (2005)	Salehi and Shahidi (1994)
100	1.0306	1.01757	1.0580	0.9904	0.96363	1.0660
200	1.7693	1.74793	1.7720	1.6094	1.55517	1.6520
300	2.2785	2.24375	2.2530	2.0069	1.92614	2.0270
400	2.6533	2.59922	2.3050	2.2923	2.18652	2.3050
500	2.9363	2.86978	2.8770	2.5142	2.38495	2.5270

Table 6. Comparison of Radial Stress Resultants for Nonlinear Bending of Solid Sector Plates

$P_z/(Eh^4/r_o^4)$	$N_r r_o^2/(Eh^3)$					
	$h/r_o = 0.05$			$h/r_o = 0.1$		
	Present	Nath et al. (2005)	Salehi and Shahidi (1994)	Present	Nath et al. (2005)	Salehi and Shahidi (1994)
100	0.6823	0.69078	0.7174	0.9552	0.96666	1.0317
200	2.1412	2.17332	2.1970	2.7186	2.74887	2.9260
300	3.7743	3.82799	3.8300	4.5187	4.56343	4.8490
400	5.4003	5.45819	5.4470	6.2303	6.28438	6.6660
500	6.9527	7.02032	7.0110	7.8480	7.90757	8.3750

Table 7. Comparison of Circumferential Stress Resultants for Nonlinear Bending of Solid Sector Plates

$P_z/(Eh^4/r_o^4)$	$N_\theta r_o^2/(Eh^3)$					
	$h/r_o = 0.05$			$h/r_o = 0.1$		
	Present	Nath et al. (2005)	Salehi and Shahidi (1994)	Present	Nath et al. (2005)	Salehi and Shahidi (1994)
100	0.7147	0.71646	0.7000	1.0048	1.00727	0.9424
200	2.2503	2.25075	2.1260	2.8624	2.86322	2.5620
300	3.9448	3.95698	3.6680	4.7607	4.75168	4.1720
400	5.6670	5.63052	5.1710	6.5665	6.54178	5.6880
500	7.2990	7.22635	6.6060	8.2738	8.22950	7.1110

Table 8. Material Properties for Ceramic and Metal

Materials	Properties	P_0	P_{-1}	P_1	P_2	P_3
Silicon nitride	E (Pa)	348.43×10^9	0	-3.070×10^{-4}	2.160×10^{-7}	-8.946×10^{-11}
	α (K^{-1})	5.8723×10^{-6}	0	9.095×10^{-4}	0	0
	K (W/mK)	13.723	0	-1.032×10^{-3}	5.466×10^{-7}	-7.876×10^{-11}
Stainless steel	E (Pa)	201.04×10^9	0	3.079×10^{-4}	-6.543×10^{-7}	0
	α (K^{-1})	12.330×10^{-6}	0	8.086×10^{-4}	0	0
	K (W/mK)	15.379	0	-1.264×10^{-3}	2.092×10^{-6}	-7.223×10^{-10}

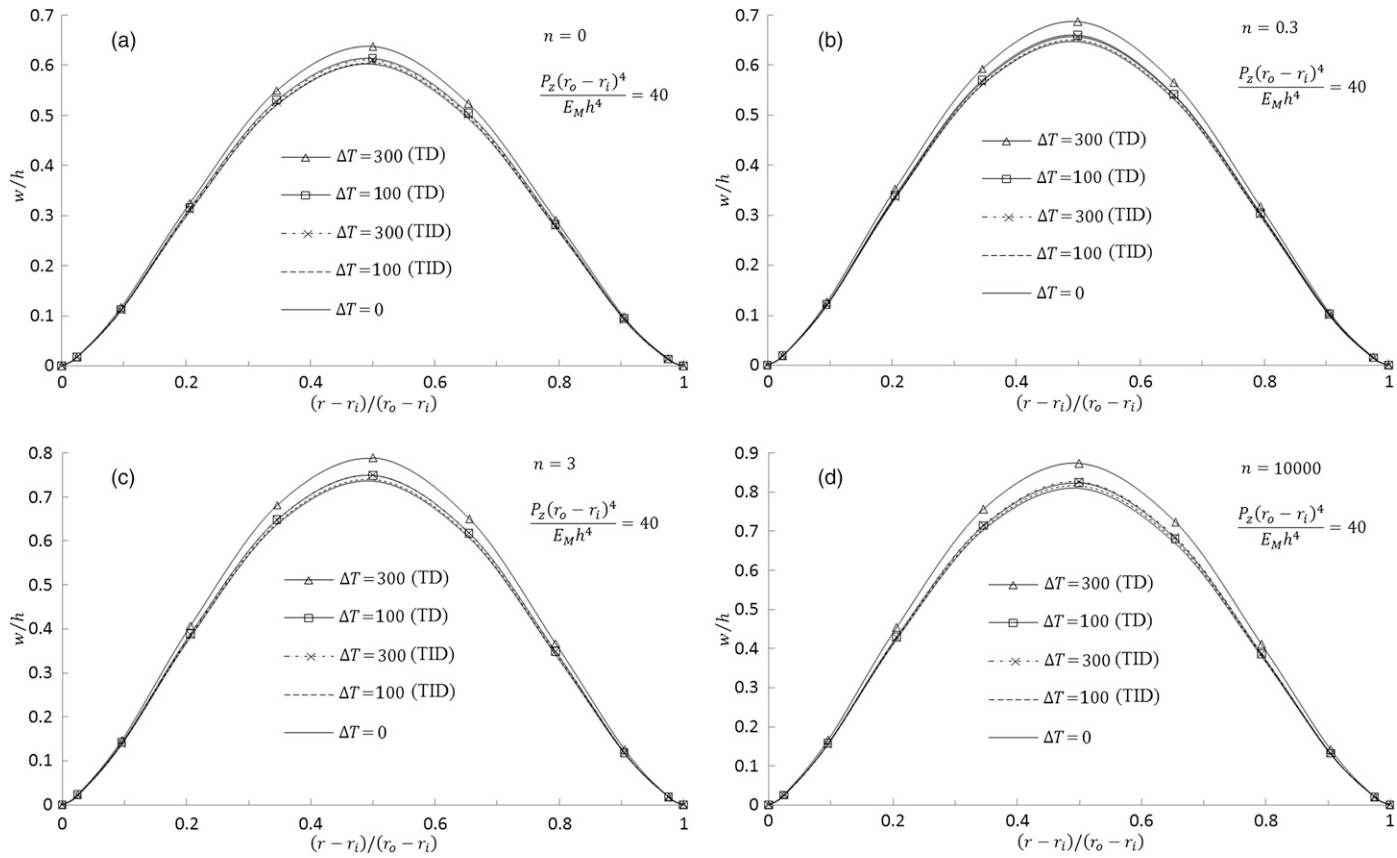

Fig. 4. Comparison of nonlinear deflections of TD and TID sector plate subjected to uniform transverse pressure and thermal loads for (a) $n = 0$; (b) $n = 0.3$; (c) $n = 3$; (d) $n = 10{,}000$

where $C_{ij}^{(m)}$ = weighting coefficients. For the first-order derivative, the weighting coefficients are calculated as

$$C_{ij}^{(1)} = \frac{M^{(1)}(x_i)}{(x_i - x_j)M^{(1)}(x_j)} \quad i, j = 1, 2, \ldots, N \tag{19a}$$

Eq. (19a) is used for $i \neq j$; however, the rest of weighting coefficients are obtained by

$$C_{ii}^{(1)} = -\sum_{j=1(j\neq i)}^{N} C_{ij}^{(1)} \quad i = 1, 2, \ldots, N \tag{19b}$$

In Eq. (19a), $M^{(1)}(x_i)$ is the first derivative of $M(x_i)$ and is defined as

$$M^{(1)}(x_k) = \prod_{j=1(j\neq k)}^{N} (x_k - x_j) \tag{20}$$

For second- and higher-order derivatives, the weighting coefficients are defined as

$$C_{ij}^{(m)} = m\left(C_{ij}^{(1)} C_{ii}^{(m-1)} - \frac{C_{ij}^{(m-1)}}{x_i - x_j}\right) \tag{21a}$$

Eq. (21a) is employed for $i \neq j$; $i, j = 1, 2, \ldots, N$; and $m = 2, 3, \ldots, N$. The remaining weighting coefficients can be obtained by

$$C_{ii}^{(m)} = -\sum_{j=1(j\neq i)}^{N} C_{ij}^{(m)} \tag{21b}$$

where $i = 1, 2, \ldots, N$ and $m = 2, 3, \ldots, N - 1$.

Numbers of grid points, as well as their positions, exert significant influence on the accuracy of the method. It is found that the optimal manner to obtain the grid points is the roots of Chebyshev polynomials.

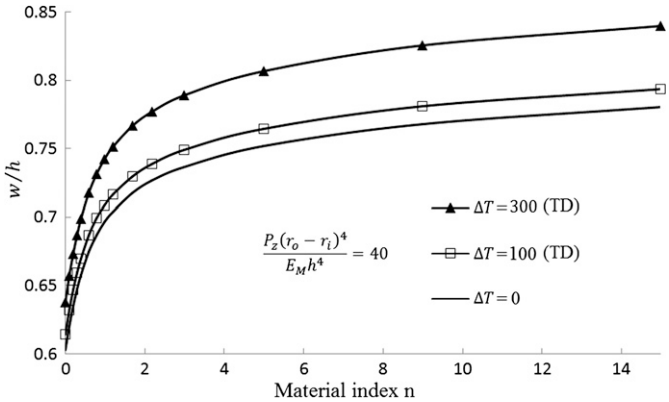

Fig. 5. Deflection versus material index for nonlinear bending of functionally graded sector plates

$$x_i = \frac{1}{2}\left\{a + b + (a-b)\cos\left[\frac{(i-1)\pi}{N-1}\right]\right\} \tag{22}$$

where $i = 1, 2, \ldots, N$. It is worth mentioning that a uniform equidistant distribution of the grid points leads to significant inaccuracy near the boundaries; thus the zeros of Chebyshev polynomials are used to consider dense nodes near the boundaries (Zong and Zhang 2009).

The first step in the solution process is to rewrite the governing equations in discretized form according to the GDQ method. For example, the discretized form of the first equation can be written as

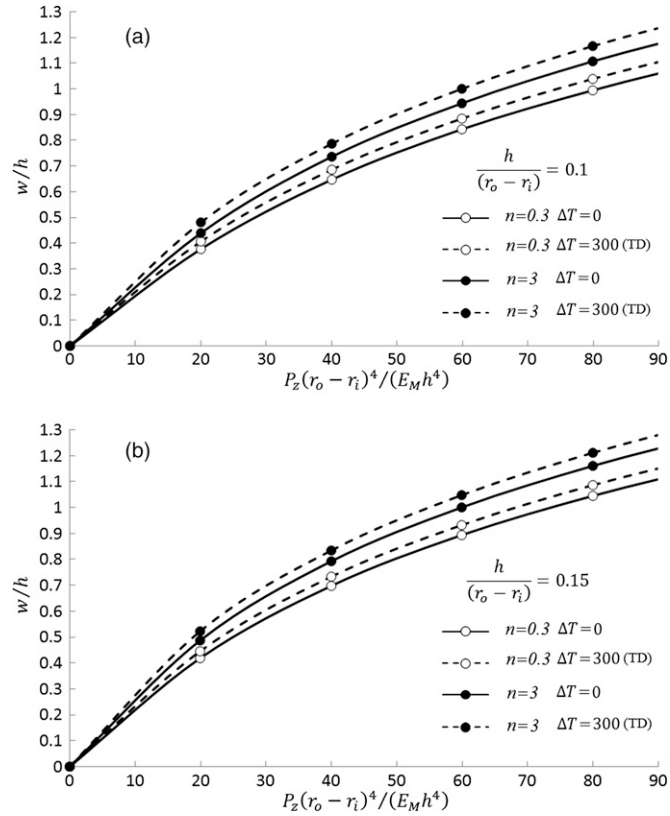

Fig. 6. Deflection versus load for nonlinear bending of functionally graded sector plates with different thickness-to-length ratios

$$\begin{aligned}
&\frac{(A_{12}+A_{33})}{r_i^2}\left(\sum_{k=1}^{N_\theta}\overline{A_{jk}}w_{ik}\right)\left(\sum_{k=1}^{N_r}A_{ik}\sum_{m=1}^{N_\theta}\overline{A_{jm}}w_{km}\right)+\frac{(A_{11}-A_{12})}{2\,r_i}\left(\sum_{k=1}^{N_r}A_{ik}w_{kj}\right)^2+\frac{(-A_{11}-A_{12})}{2r_i^3}\left(\sum_{k=1}^{N_\theta}\overline{A_{jk}}w_{ik}\right)^2\\
&+A_{11}\left(\sum_{k=1}^{N_r}A_{ik}w_{kj}\right)\left(\sum_{k=1}^{N_r}B_{ik}w_{kj}\right)+\frac{A_{33}}{r_i^2}\left(\sum_{k=1}^{N_\theta}\overline{B_{jk}}w_{ik}\right)\left(\sum_{k=1}^{N_r}A_{ik}w_{kj}\right)+A_{11}\left(\sum_{k=1}^{N_r}B_{ik}u_{kj}\right)+\frac{A_{33}}{r_i^2}\left(\sum_{k=1}^{N_\theta}\overline{B_{jk}}u_{ik}\right)\\
&+\frac{A_{11}}{r_i}\left(\sum_{k=1}^{N_r}A_{ik}u_{kj}\right)-A_{11}\frac{u_{ij}}{r_i^2}-\frac{(A_{11}+A_{33})}{r_i^2}\left(\sum_{k=1}^{N_\theta}\overline{A_{jk}}v_{ik}\right)+\frac{(A_{12}+A_{33})}{r_i}\left(\sum_{k=1}^{N_r}A_{ik}\sum_{m=1}^{N_\theta}\overline{A_{jm}}v_{km}\right)+B_{11}\left(\sum_{k=1}^{N_r}B_{ik}\varphi_{rkj}\right)\\
&+\frac{B_{33}}{r_i^2}\left(\sum_{k=1}^{N_\theta}\overline{B_{jk}}\varphi_{rik}\right)+\frac{B_{11}}{r_i}\left(\sum_{k=1}^{N_r}A_{ik}\varphi_{rkj}\right)-B_{11}\frac{\varphi_{rij}}{r_i^2}-\frac{(B_{11}+B_{33})}{r_i^2}\left(\sum_{k=1}^{N_\theta}\overline{A_{jk}}\varphi_{\theta ik}\right)+\frac{(B_{12}+B_{33})}{r_i}\left(\sum_{k=1}^{N_r}A_{ik}\sum_{m=1}^{N_\theta}\overline{A_{jm}}\varphi_{\theta km}\right)=0
\end{aligned} \tag{23}$$

where $i = 1, 2, \ldots, N$; $j = 1, 2, \ldots, N_\theta$; A_{pq} and B_{pq} = weighting coefficients for the first- and second-order derivatives with respect to r, respectively; and $\overline{A_{pq}}$ and $\overline{B_{pq}}$ = weighting coefficients of the first- and second-order derivatives with respect to θ, respectively. The other equations are discretized in an analogous manner.

Results and Discussion

To verify the accuracy of the results obtained by the GDQ method, some results are compared with the results of other numerical methods. As the first example, an isotropic fully clamped annular sector plate with constant thickness of $h = 0.002$ m, total angle $\alpha = \pi/3$, Young's modulus of $E = 207$ GPa, and Poisson's ratio of $\nu = 0.3$ subjected to a uniform pressure P_z is considered. Linear maximum dimensionless deflections of the plate for various ratios of inner to outer radii are tabulated in Table 1. This table shows that the results obtained by the GDQ method are in a good agreement with the results reported by Aghdam et al. (2007) and Mousavi and Tahani (2012).

To demonstrate the accuracy and validity of these results in linear bending analysis of functionally graded sector plates, a fully

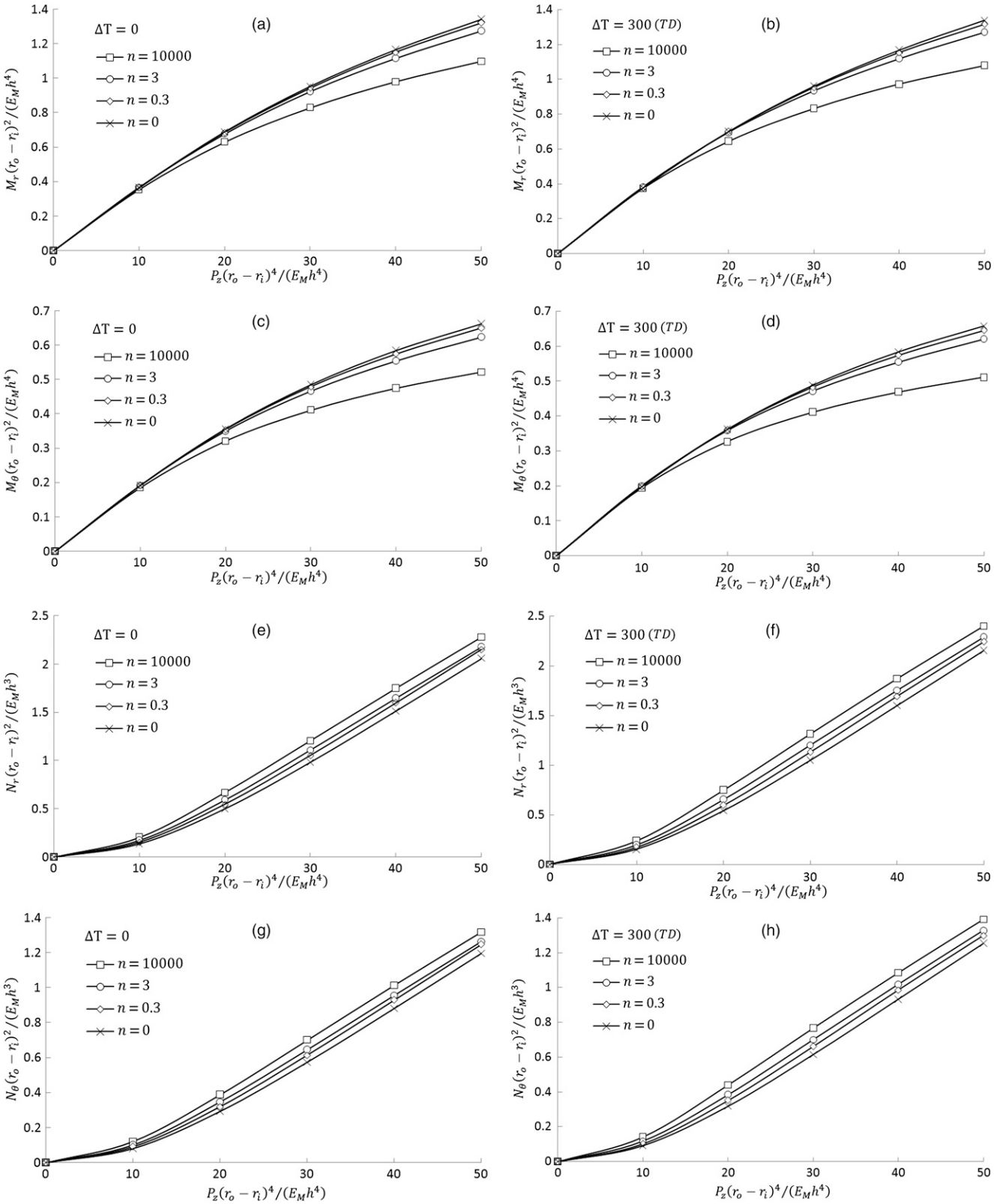

Fig. 7. Stress and moment resultants at the middle point versus pressure for nonlinear bending of functionally graded sector plates with and without thermal load

clamped functionally graded solid sector plate (i.e., $r_i = 0$) with total angle $\alpha = \pi/3$, outer radius $r_o = 5$ m, constant thickness $h = 0.2$ m, and mechanical properties given in Table 2 is considered. It is assumed that the plate is subjected to a uniform pressure P_z. The deflections along the radial centerline $(r, \alpha/2)$ of the functionally graded sector plate for $n = 2$ are compared with the results of Aghdam et al. (2012) in Fig. 3. It can be concluded from Fig. 3 that the results of the GDQ method are in excellent agreement with those of the extended Kantorovich method solution.

As part of validation of the present method in nonlinear analysis of sector plates, a fully clamped isotropic solid sector plate with total angle $\alpha = \pi/3$ and Poisson's ratio $\nu = 0.3$ subjected to a downward uniform pressure P_z is considered. Normalized deflection, moment resultants, and stress resultants at point $[(r - r_i)/(r_o - r_i) = 0.647, \theta = \pi/6]$ for various numbers of normalized loads are compared with the results of Salehi and Shahidi (1994) and Nath et al. (2005) in Tables 3–7. Given that in the GDQ method, positions of the grid points are roots of Chebyshev polynomials, these values at point $[(r - r_i)/(r_o - r_i) = 0.647, \theta = \pi/6]$ are found by passing a polynomial through values of each grid point and finding the value of that polynomial at $[(r - r_i)/(r_o - r_i) = 0.647, \theta = \pi/6]$.

In the remaining parts of the present work, the effects of mechanical and thermal loads on functionally graded sector plates are studied in more detail. The constituent materials of functionally graded plates are assumed to be silicon nitride and stainless steel, referred to as Si_3N_4/SUS304. The mechanical and thermal properties such as P are expressed as a nonlinear function of temperature (Touloukian 1967) as

$$P = P_0\left(P_{-1}T^{-1} + 1 + P_1T + P_2T^2 + P_3T^3\right) \tag{24}$$

where

$$T = T_0 + \Delta T \tag{25}$$

where ΔT = difference between temperature of upper surface and lower surface ($\Delta T = T_U - T_L$) and $T_0 = 300$ K (room temperature); $P_i\,(i = -1, 0, 1, 2, 3)$ = coefficients of temperature T(K) and are unique for each constituent material. Young's modulus, the thermal expansion coefficient, and thermal conductivity are assumed to depend on temperature and are obtained by Eq. (24). Furthermore, Poisson's ratio is considered to be a constant and $\nu = 0.28$ (Shen and Wang 2010). Coefficients of temperature for the constituent materials are taken from Reddy and Chin (1998) and are given in Table 8.

The results presented herein are for an annular sector plate with $h/(r_o - r_i) = 0.1$, $r_i/r_o = 0.5$, and total angle $\alpha = \pi/3$ and subjected to a uniform pressure $P_z(r_o - r_i)^4/(E_M h^4) = 40$, unless mentioned otherwise. It should be mentioned that E_M in the dimensionless pressure is the elasticity modulus of stainless steel at $T = 300$ K. The lower surface of the plate is held at room temperature for all cases; thus $\Delta T_L = 0$, and for the upper surface, $\Delta T_U = \Delta T$.

Fig. 4 shows the deflection along centerline $(r, \alpha/2)$ for nonlinear bending of functionally graded annular sector plates with various values of n subjected to a uniform pressure $P_z(r_o - r_i)^4/(E_M h^4) = 40$ and thermal loads. The material properties are assumed to be temperature-dependent (TD) and temperature-independent (TID). Properties of the TID materials are obtained by Eq. (24) at $T = 300$ K. It can be seen from these figures that thermal loads do not have significant influence on deflection of a TID sector plate with clamped boundary conditions; however, a TD sector plate shows

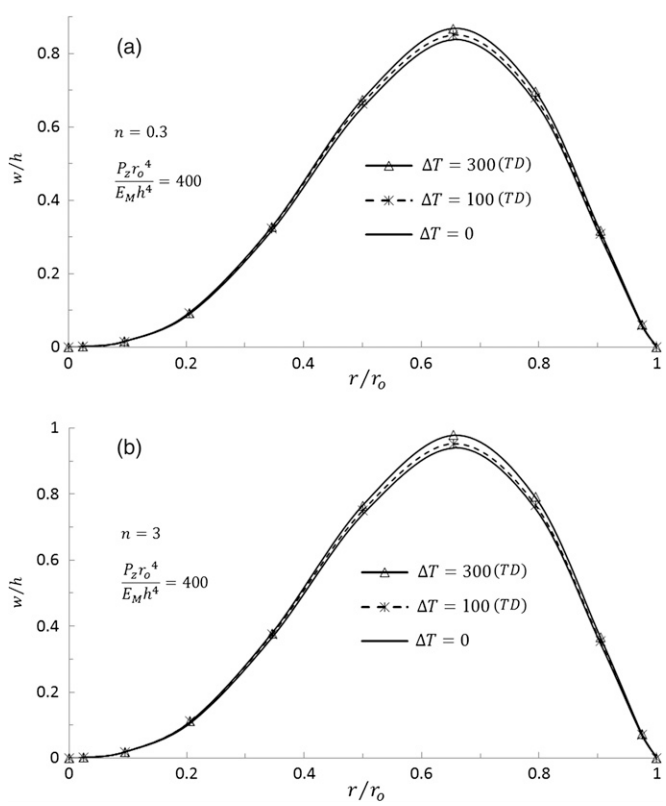

Fig. 8. Deflection along radial centerline for nonlinear bending of solid sector plate

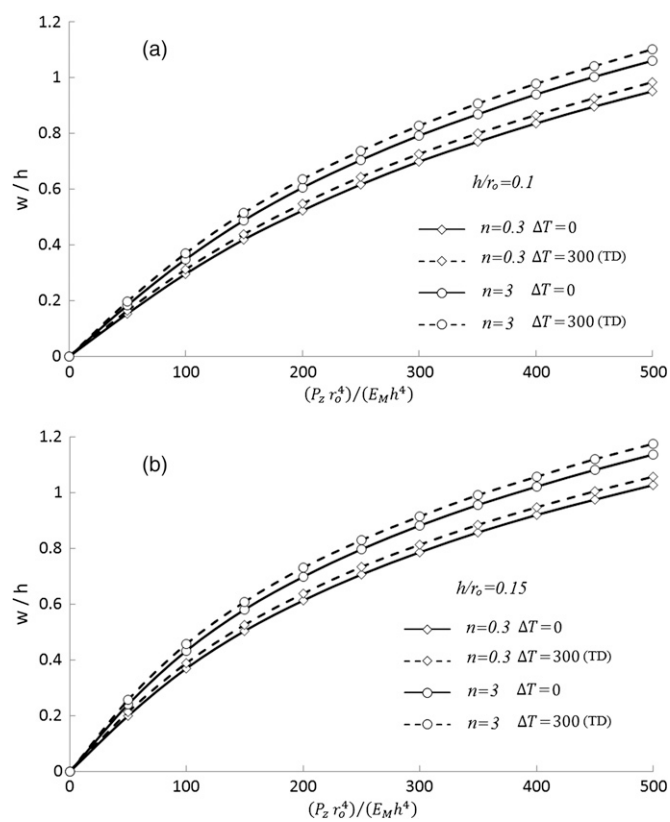

Fig. 9. Deflection versus load at $r/r_o = 0.647$ for nonlinear bending of functionally graded solid sector plates with different thickness-to-radius ratios

considerable deflection owing to thermal loads. Furthermore, higher deflection is observed as the volume fraction of the Si_3N_4 reduces by increasing n.

The effects of the material index n on the deflections of sector plates are shown in Fig. 5. This figure shows the nonlinear deflection at the middle point $[(r_o + r_i)/2, \alpha/2]$ of sector plates under a uniform pressure and thermal loads for various values of n. As expected, the plates display more deflection by increasing material index n. Moreover, thermal loads cause more deflection for large values of material index. Deflection of functionally graded plates increases more rapidly when material index n rises from 0 to 5. However, for $n > 5$, the effects of n become less significant.

To study the effects of thickness-to-length ratios and nonlinear responses of plates to various values of pressure, two functionally graded sector plates with thickness-to-length ratios of $h/(r_o - r_i) = 0.1$ and $h/(r_o - r_i) = 0.15$ are considered. The nonlinear deflections of the plates at the middle point $[(r_o + r_i)/2, \alpha/2]$ versus load are depicted in Fig. 6. As expected, these results show that the dimensionless middle deflections are decreased by decreasing thickness-to-length ratio $h/(r_o - r_i)$.

Stress and moment resultants at the middle point $[(r_o + r_i)/2, \alpha/2]$ for nonlinear bending of functionally graded sector plates with and without thermal loads versus pressure for different values of material indices are shown in Fig. 7. It can be concluded from these figures that the moment and stress resultants increase as the pressure increases, and the effects of pressure on the radial moment and stress resultants are more than those of the circumferential moment and stress resultants. In addition, the effects of thermal loads on stress resultants are more than those of the moment resultants. Furthermore, the effect of changing material index n on the moment resultants of the functionally graded plates is not so significant. Mousavi and Tahani (2012) also showed that change of material index leads to significant changes in deflection; however, it has a negligible effect on in-plane stresses components.

Solid Sector Plates

A fully clamped functionally graded solid sector plate with $h/r_o = 0.1$ and total angle $\alpha = \pi/3$ with the material properties given in Table 8 subjected to a uniform mechanical load of $(P_z r_o^4)/(E_M h^4) = 400$ and various thermal loads is considered. Poisson's ratio is assumed to be a constant $\nu = 0.28$. The resulting nonlinear deflections along the centerline $(r, \alpha/2)$ of the plate for different material indices are compared with each other in Fig. 8. It can be seen that the thermal loads have more influence on the deflection of plates with large material indices, and thus plates exhibit more deflection by increasing the material index.

Furthermore, the effects of thickness-to-radius ratios and the nonlinear response of solid sector plates to various pressures are studied in Fig. 9. This figure shows the deflection of functionally graded solid sector plates at point $r/r_o = 0.647$ and $\theta = \alpha/2$ for $h/r_o = 0.1$ and 0.15. As expected, by increasing the thickness-to-radius ratio h/r_o, the nondimensional deflections increase. It also can be seen that as with previous results, increasing thermal loads as well as the material index n leads to a rise in deflection.

Conclusions

The effects of thermomechanical loads on the nonlinear response of clamped functionally graded annular sector plates were investigated. Employing the principle of minimum total potential energy, the governing equations were derived base on the FSDT. The system of five nonlinear partial differential equations was solved with the GDQ method in conjunction with the Newton-Raphson iterative scheme. The accuracy of this method was verified by comparing the results with those existing in the literature. It was found that the effect of thermal loads on the deflection of TID plates is negligible versus that of plates with TD material properties. Furthermore, plates show more deflection as the volume fraction of ceramic decreases by increasing n; however, a change in material index imposes negligible effect on moment and stress resultants.

References

Aghdam, M. M., Mohammadi, M., and Erfanian, V. (2007). "Bending analysis of thin annular sector plates using extended Kantorovich method." *Thin-Walled Struct.*, 45(12), 983–990.

Aghdam, M. M., Shahmansouri, N., and Mohammadi, M. (2012). "Extended Kantorovich method for static analysis of moderately thick functionally graded sector plates." *Math. Comput. Simul.*, 86, 118–130.

Andakhshideh, A., Maleki, S., and Aghdam, M. M. (2010). "Non-linear bending analysis of laminated sector plates using generalized differential quadrature." *Compos. Struct.*, 92(9), 2258–2264.

Bellman, R., and Casti, J. (1971). "Differential quadrature and long-term integration." *J. Math. Anal. Appl.*, 34(2), 235–238.

Chi, S. H., and Chung, Y. L. (2006a). "Mechanical behavior of functionally graded material plates under transverse load. I: Analysis." *Int. J. Solids Struct.*, 43(13), 3657–3674.

Chi, S. H., and Chung, Y. L. (2006b). "Mechanical behavior of functionally graded material plates under transverse load. II: Numerical results." *Int. J. Solids Struct.*, 43(13), 3675–3691.

Hosseini-Hashemi, S. H., Akhavan, H., Rokni Damavandi Taher, H., Daemi, N., and Alibeigloo, A. (2010a). "Differential quadrature analysis of functionally graded circular and annular sector plates on elastic foundation." *Mater. Des.*, 31(4), 1871–1880.

Hosseini-Hashemi, S. H., Rokni Damavandi Taher, H., and Akhavan, H. (2010b). "Vibration analysis of radially FGM sectorial plates of variable thickness on elastic foundations." *Compos. Struct.*, 92(7), 1734–1743.

Jomehzadeh, E., Saidi, A. R., and Atashipour, S. R. (2009). "An analytical approach for stress analysis of functionally graded annular sector plates." *Mater. Des.*, 30(9), 3679–3685.

Koizumi, M. (1993). "The concept of FGM." *Ceram. Trans. Funct. Grad. Mater.*, 34, 3–10.

Mousavi, S. M., and Tahani, M. (2012). "Analytical solution for bending of moderately thick radially functionally graded sector plates with general boundary conditions using multi-term extended Kantorovich method." *Compos. Part B Eng.*, 43(3), 1405–1416.

Na, K.-S., and Kim, J. H. (2006). "Nonlinear bending response of functionally graded plates under thermal loads." *J. Therm. Stresses*, 29(3), 245–261.

Nádai, A. (1915). "Über das Ausbeulen von Kreisförmigen Platten." Zeitschrift des Vereins Deutscher Ingenieure, 59, 169–174.

Naderi, A., and Saidi, A. R. (2011). "Exact solution for stability analysis of moderately thick functionally graded sector plates on elastic foundation." *Compos. Struct.*, 93(2), 629–638.

Nath, Y., Sharda, H. B., and Sharma, A. (2005). "Non-linear analysis of moderately thick sector plates." *Commun. Nonlinear Sci. Numer. Simul.*, 10(7), 765–778.

Nguyen, T. K., Sab, K., and Bonnet, G. (2008). "First-order shear deformation plate models for functionally graded materials." *Compos. Struct.*, 83(1), 25–36.

Praveen, G. N., and Reddy, J. N. (1998). "Nonlinear transient thermoelastic analysis of functionally graded ceramic-metal plates." *Int. J. Solids Struct.*, 35(33), 4457–4476.

Reddy, J. N. (2002). *Energy principles and variational methods in applied methods in applied mechanics*, 2nd Ed., Wiley, New York.

Reddy, J. N., and Chin, C. D. (1998). "Thermomechanical analysis of functionally graded cylinders and plates." *J. Therm. Stresses*, 21(6), 593–626.

Saidi, A. R., and Hasani Baferani, A. (2010). "Thermal buckling analysis of moderately thick functionally graded annular sector plates." *Compos. Struct.*, 92(7), 1744–1752.

Salehi, M., and Shahidi, A. (1994). "Large deflection analysis of elastic sector Mindlin plates." *Comput. Struct.*, 52(5), 987–998.

Salehi, M., and Turvey, G. J. (1991). "Elastic large deflection response of annular sector plates: A comparison of DR finite-difference, finite element and other numerical solutions." *Comput. Struct.*, 40(5), 1267–1278.

Shen, H. S., and Wang, Z. X. (2010). "Nonlinear bending of FGM plates subjected to combined loading and resting on elastic foundations." *Compos. Struct.*, 92(10), 2517–2524.

Shu, C., and Richards, B. E. (1992). "Application of generalized differential quadrature to solve two-dimensional incompressible Navier-Stokes equations." *Int. J. Numer. Methods Fluids*, 15(7), 791–798.

Touloukian, Y. S. (1967). *Thermophysical properties of high temperature solid materials*, Macmillan, New York.

Wang, C. M., Reddy, J. N., and Lee, K. H. (2000). *Shear deformable beams and plates: Relationships with classical solutions*, 1st Ed., Elsevier Science, New York.

Yamanoushi, M., Koizumi, M., Hiraii, T., and Shiota, I., eds. (1990). "Overall view of the P/M fabrication of functionally gradient materials." *Proc.*, *1st Int. Symp. on Functionally Gradient Materials*, Functionally Gradient Materials Forum, Japan, 107–113.

Yang, J., and Shen, H. S. (2003). "Nonlinear bending analysis of shear deformable functionally graded plates subjected to thermo-mechanical loads under various boundary conditions." *Compos. Part B Eng.*, 34(2), 103–115.

Zong, Z., and Zhang, Y. (2009). *Advanced differential quadrature methods*, CRC Press, Boca Raton, FL.